Evaluation of the in vitro anticancer activity of cyclometalated half-sandwich rhodium and iridium complexes coordinated to naphthaldimine-based poly(propyleneimine) dendritic scaf...

ARTICLE *in* JOURNAL OF ORGANOMETALLIC CHEMISTRY · DECEMBER 2014

Impact Factor: 2.17 · DOI: 10.1016/j.jorganchem.2014.10.003

Journal of Organometallic Chemistry 774 (2014) 79–85

Contents lists available at ScienceDirect

Journal of Organometallic Chemistry

journal homepage: www.elsevier.com/locate/jorganchem

Evaluation of the *in vitro* anticancer activity of cyclometalated half-sandwich rhodium and iridium complexes coordinated to naphthaldimine-based poly(propyleneimine) dendritic scaffolds

Lara C. Sudding [a], Richard Payne [a], Preshendren Govender [a], Fabio Edafe [b], Catherine M. Clavel [b], Paul J. Dyson [b], Bruno Therrien [c], Gregory S. Smith [a, *]

[a] Department of Chemistry, University of Cape Town, Private Bag, Rondebosch 7701, South Africa
[b] Institut des Sciences et Ingénierie Chimiques, Ecole Polytechnique Fédérale de Lausanne (EPFL), CH1015 Lausanne, Switzerland
[c] Institute of Chemistry, University of Neuchatel, 51 Ave de Bellevaux, CH-2000 Neuchatel, Switzerland

ARTICLE INFO

Article history:
Received 8 August 2014
Received in revised form
23 September 2014
Accepted 1 October 2014
Available online 12 October 2014

Keywords:
Bioorganometallic chemistry
Cyclometalated
Rhodium
Iridium
Metallodendrimers
Anticancer drugs

ABSTRACT

The development of cyclometalated rhodium and iridium complexes from first- and second-generation naphthaldimine-based poly(propyleneimine) dendrimer scaffolds of the type, DAB-$(NH_2)_n$ (where $n = 4$ or 8, DAB = diaminobutane) has been accomplished. Four metallodendrimers were synthesised, viz. $(Cp^*MCl)_4\mathbf{G^n}$ (**1**–**4**), by first reacting DAB-$(NH_2)_n$ with napththaldehyde and subsequently metallating the Schiff-base dendrimers with the dimers $[Cp^*MCl_2]_2$ (where M = Rh or Ir). Related mononuclear complexes $[Cp^*MCl(L)]$ (L = naphthaldimine) (**5**–**6**) were obtained in a similar manner. The molecular structures of **5** and **6** have been determined by single-crystal X-ray diffraction analysis and the *in vitro* anticancer activities of **1**–**6** were evaluated against the A2780 and A2780cisR human ovarian carcinoma cell lines.

Introduction

The discovery of cisplatin as an anticancer transition metal-based drug pioneered research into metal-based drug discovery in the field of medicinal inorganic chemistry, and metal complexes are currently an important resource for the generation of chemical diversity in the search for novel diagnostic and therapeutic agents [1–11]. Despite being used in about 50% of all cancer treatment regimens, cisplatin and other platinum-based drugs found in the clinic are poorly selective and produce several undesirable side-effects [12,13]. It is these side-effects that limit the dose that can be administered to a patient, thus allowing certain tumours to develop acquired resistance mechanisms. Research now focuses its attentions on the development of new metal-based drugs with fewer side-effects and with different mechanisms of action. Among the transition metals, ruthenium appears to be the most promising candidate [14–18]. It possesses an octahedral coordination geometry, thus having two additional binding sites in comparison with Pt(II) metal-based drugs. The redox chemistry of ruthenium is rich and compatible with biological media. The overall toxicity of ruthenium is lower than platinum, thus allowing higher doses for treatment.

Metal-based drugs containing rhodium and iridium are explored to a lesser extent and recent work suggests that these compounds lend themselves to development as novel anticancer drugs [19–29]. More recently, researchers have turned their attention to cyclometalated complexes in which a chelating ring contains a strong M–C sigma bond. The biological properties of the cyclometalated complexes can be tweaked by modification of the anionic cyclometalated ligand or through ancillary ligands around the metal centre. Improved cytotoxicity and pharmacokinetics have been observed for many complexes ascribed to their greater stability afforded by this class of ligand [30,31].

The concept of multinuclearity is an innovative strategy often resulting in improved biological activity with respect to mononuclear compounds [32–35], which could be attributed to favourable modulation of the stability, solubility and/or lipophilicity of the organometallic scaffolds. Since the development of the trinuclear platinum-based anticancer drug, BBR3464 [*trans*, *trans*, *trans*-

* Corresponding author. Tel.: +27 21 6505279; fax: +27 21 6505195.
E-mail address: gregory.smith@uct.ac.za (G.S. Smith).

http://dx.doi.org/10.1016/j.jorganchem.2014.10.003
0022-328X/

$(NH_3)_2$–Pt(Cl)
$NH_2(CH_2)_6NH_2Pt(NH_3)_2NH_2(CH_2)_6NH_2Pt$–$(NH_3)_2(Cl)][NO_3]_4$ [36], the concept of multinuclearity has not been extensively explored in the development of new anticancer agents. An attractive strategy used to exploit this concept makes use of macromolecules such as dendrimers.

Metallodendrimers, i.e. metal-containing dendritic macromolecules, have recently found potential as diagnostic agents and as chemotherapeutics [37]. In line with this strategy, the multivalent/multinuclear nature of metallodendrimers can enhance interactions between a dendrimer-drug conjugate and a target bearing multiple receptors. In this respect, we have recently reported the synthesis of a series of metallodendrimers, containing ruthenium-arene and osmium-arene functionalities located on the periphery of the dendritic scaffold [32,33,38,39]. A cationic 32-armed ruthenium-*p*-cymene-PTA functionalised metallodendrimer was shown to have antiproliferative activity in the nanomolar range (A2780, human ovarian cancer cell line) [39]. Recently, we have reported half-sandwich rhodium and iridium metallodendrimers which displayed moderate to good activity *in vitro* [40]. Indeed, the biological properties of numerous polymetallic compounds have been reported in the literature [41–47].

As an extension of the above work, we have now synthesised a series of polynuclear half-sandwich cyclometalated rhodium and iridium complexes, based on a naphthaldimine poly(propyleneimine) (PPI) dendritic scaffold. The cytotoxicities of the rhodium and iridium metallodendrimers have been established using ovarian A2780 (cisplatin-sensitive) and A2780cisR (cisplatin-resistant) cancer cell lines and a non-cancerous HEK (human embryonic kidney) cell line.

Results and discussion

*Synthesis and characterisation of naphthaldimine-functionalised (**G¹**, **G²**) dendrimers*

The naphthaldimine-functionalised first- and second-generation dendrimers (**G¹**–**G²**) were synthesised by the reaction of naphthaldehyde with DAB-$(NH_2)_n$ (where $n = 4$ or 8 for **G¹** and **G²** respectively) (Fig. 1). The dendrimers were isolated as white solids in moderate yields and are readily soluble in dichloromethane, chloroform and acetone.

In the ^{1}H NMR spectra of both dendrimers **G¹** and **G²** there is a characteristic imine peak at around 8.4 ppm. A key feature in the ^{1}H NMR spectrum is the downfield position of the triplet corresponding to the protons on the carbon atom adjacent to the imine nitrogen, appearing around 3.6 ppm for **G¹** and **G²**. ^{13}C{^{1}H} NMR spectra indicate the presence of the characteristic imine carbon peak at around 161 ppm for **G¹** and **G²**. To further confirm that the Schiff-base reaction occurred, IR spectroscopy shows imine absorption bands at 1639 cm^{-1} for both the first- and second-generation naphthaldimine dendrimers **G¹** and **G²**.

*Synthesis and characterisation of rhodium and iridium metallodendrimers **1**–**4***

The dinuclear pentamethylcyclopentadienyl (Cp*) rhodium or iridium dimers $[Cp^*MCl_2]_2$ (M = Rh or Ir) were reacted with **G¹** and **G²** at room temperature in the presence of sodium acetate to yield the neutral tetranuclear (**1**–**2**) and octanuclear (**3**–**4**) rhodium and iridium metallodendrimers (Scheme 1). The yellow–orange compounds (**1**–**4**) were isolated as air-stable solids in moderate yields. The complexes are soluble in organic solvents such as dichloromethane, chloroform, ethanol, dimethylsulfoxide and acetone.

The ^{1}H NMR spectra of the three metallodendrimers reveal upfield shifts of the imine resonance from ~8.4 ppm in the metal-free dendrimers **G¹** and **G²** to ~8.0 ppm for **1** and **2**, and ~8.3 ppm for **3** and **4**. This confirms that the imine bond is still intact and that there is coordination of the metal centre to the imine nitrogen. There is significant broadening of all the peaks in the NMR spectra, especially observed for the peripheral end-groups, due to the multivalent nature of the dendrimer and on the given NMR timescale, this averages out to a broadened signal over the same chemical shift. In all the complexes **1**–**4**, there is a characteristic broad multiplet between 3.96 and 4.12 ppm in the ^{1}H NMR spectra that corresponds to the protons on the carbon adjacent to the imine nitrogen. For the Rh(III) complex **1**, this signal appears as two broad peaks which is expected as these two protons are in different environments due to diastereotopicity, being adjacent to the chiral metal centre, whereas for the Ir(III) complexes **2** and **4**, the two signals coalesce and appear as one broad peak.

In the ^{13}C{^{1}H} NMR spectrum there is a carbon peak furthest downfield in each complex, at 133.37 and 136.60 ppm for complexes **1** and **2**, respectively, which corresponds to the imine carbon.

IR spectroscopy was used to confirm whether there had been coordination of the dendrimer to the metal centre. The IR spectra of metallodendrimers **1**–**4** reveal imine absorption peaks at lower frequencies around 1600 cm^{-1} (for **2** and **4**) and around 1610 cm^{-1} (for **1** and **3**), compared to that of the metal-free dendrimers (**G¹** and **G²**) at around 1639 cm^{-1}.

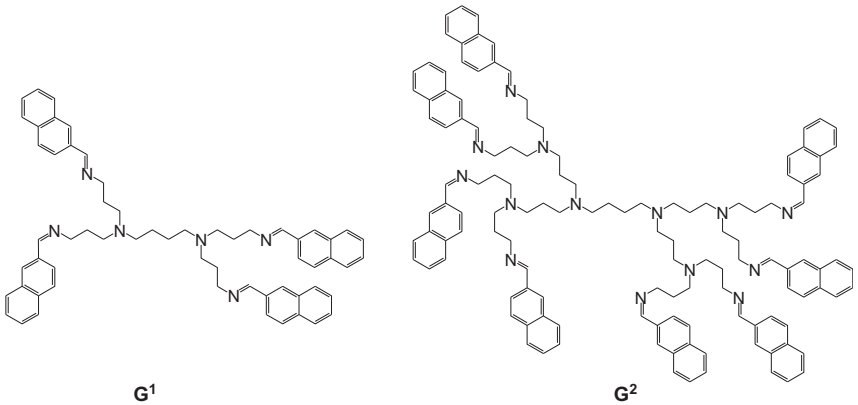

Fig. 1. First- and second-generation of naphthaldimine (**G¹**, **G²**) dendrimers.

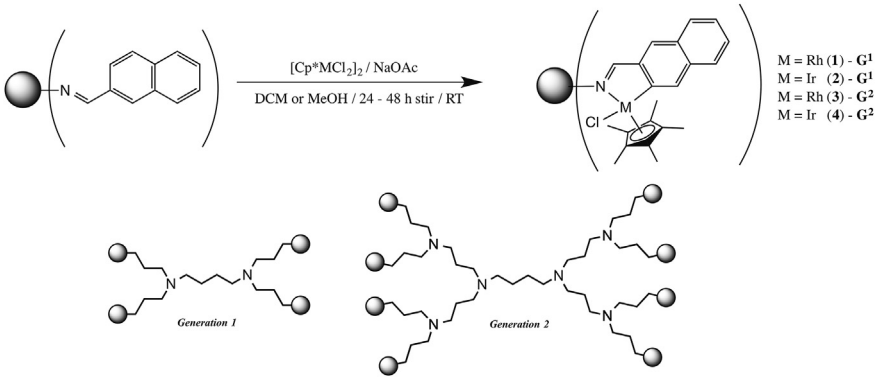

Scheme 1. Tetra- and octanuclear rhodium and iridium metallodendrimers **1**–**4**.

High resolution-ESI mass spectrometry was used for metallodendrimers (**1**–**4**), to confirm that the desired products were obtained. The results for the Rh(III) complex **1** show the appearance of base peaks at 1959.4369 and 1923.4751 *m*/*z* which correspond to the pseudomolecular ion peak as well as a peak corresponding to the loss of a chloride ligand (1959.52 g/mol). In the case of the Ir(III) complex **2**, there is a base peak at 1159.3489 *m*/*z* corresponding to the $[M+2H]^{2+}$ ion as well as a peak at 1122.3962 *m*/*z* corresponding to the $[M-2Cl]^{2+}$ ion (2316.78 g/mol).

*Synthesis and characterisation of mononuclear rhodium and iridium complexes (**5**,**6**)*

Analogous mononuclear rhodium and iridium complexes (**5**–**6**) were prepared for comparison as models of the more complex macromolecular structures. These were synthesised by reacting the naphthaldimine ligand (**L1**) with the dinuclear Cp* rhodium or iridium dimers $[Cp^*MCl_2]_2$ (M = Rh or Ir) in dichloromethane at room temperature (Scheme 2).

The mononuclear metal complexes **5**–**6** were isolated as yellow–orange solids in moderate yields. They are air-stable and soluble in methanol, ethanol, acetone, dichloromethane and chloroform. The ^{1}H NMR spectra of each metal complex **5** and **6** indicate coordination of the metal centre to the ligand in a bidentate fashion with an upfield shift of the imine peak in the Rh(III) complex **5** from 8.43 ppm (for **L1**) to 8.23 ppm, whilst there is no observable shift of the imine peak in the Ir(III) complex **6**. ^{13}C{^{1}H} NMR spectroscopy show characteristic carbon peaks at about 145 ppm for both complexes, corresponding to the imine carbon, further upfield in comparison with the imine carbon resonance in the metal-free ligand **L1** at about 160 ppm. The IR spectra for the complexes **5** and **6** indicate a shift of the imine absorption band to a lower frequency of 1610 cm^{-1} for the Rh(III) complex **5** and 1603 cm^{-1} for the Ir(III) complex **6**. The ESI-mass spectrum of the each complex show base peaks corresponding to the pseudomolecular ion with the loss of the chloride ion, $[M - Cl]^+$.

*X-ray diffraction studies of complexes **5** and **6***

X-ray quality single crystals for **5** were obtained from a toluene/hexane mixture, while for **6**, crystals were obtained from a methanol/hexane mixture. The molecular structures of **5** and **6** confirm the characteristic pseudo-tetrahedral "piano-stool" geometry with a η^5-coordination of the Cp* to the metal centre. This coordination forms the 'seat' of the piano-stool and the remaining bonds of the C,N chelate and the chloride form the 'legs' of the "piano-stool" (Fig. 2). As emphasized in Fig. 2, the complexes are chiral, which supports the diastereotopic nature of the ^{1}H NMR signals.

Complex **5** crystallizes with a molecule of toluene in the monoclinic space group $P\,2_1/n$, while complex **6** crystallizes in the orthorhombic space group $P\,2_12_12_1$. The distances between the metal centres and the aromatic carbon atoms range between 2.159(3) and 2.275(3) Å for the rhodium derivative and between 2.140(6) and 2.263(6) for the iridium analogue. The bond length between the metal centre and the chloride ligand is 2.3984(8) Å for the Rh(III) complex, and 2.391(2) Å for the Ir(III) complex. In both complexes, the metal nitrogen-imine bond lengths are comparable at 2.097(3) and 2.088(5) Å, respectively. However, the Rh–C1 bond length is shorter [2.030(3) Å] than the Ir–C1 bond length [2.046(7) Å]. The crystallographic details for both structures are given in Table 1.

*Anticancer activity of complexes **1**–**6***

A preliminary investigation of the biological activity of the aforementioned metallodendrimers and mononuclear compounds was undertaken and the antiproliferative activity of **1**–**6** was evaluated *in vitro* in the A2780 and A2780cisR ovarian cancer cell lines using the MTT assay which measures mitochondrial dehydrogenase activity as an indication of cell viability. The IC_{50} values (inhibition of cancer cell growth at the 50% level) are listed in Table 2 and were calculated as an average over two independent experiments.

The polynuclear compounds generally display moderate to high antiproliferative activity in the A2780 (cisplatin-sensitive) and

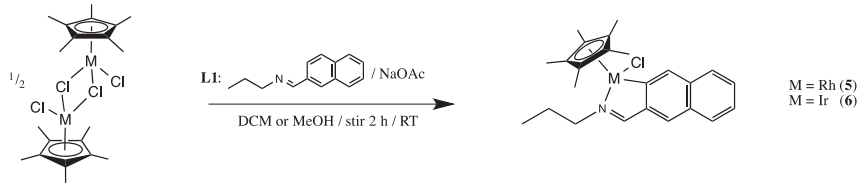

Scheme 2. Synthesis of the mononuclear rhodium and iridium complexes **5**–**6**.

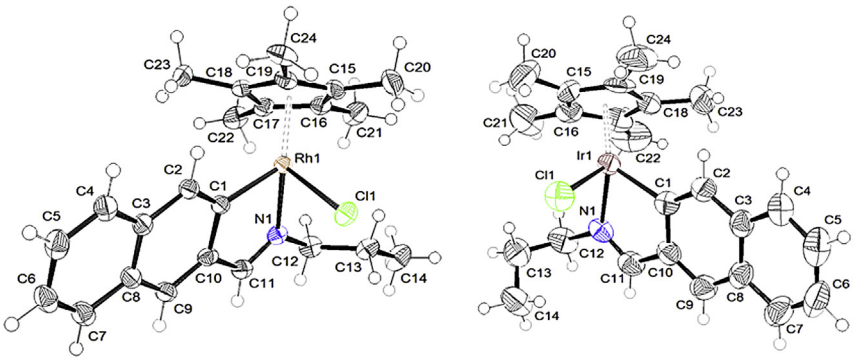

Fig. 2. Molecular structures of the mononuclear complexes **5** and **6**. The solvate molecule in **5** has been omitted for clarity, thermal ellipsoids are drawn at the 50% probability level.

Table 1
Crystallographic parameters for complexes **5**·toluene and **6**.

	5·toluene	**6**
Chemical formula	$C_{31}H_{29}ClNRh$	$C_{24}H_{29}ClIrN$
Formula weight	553.91	559.13
Crystal system	Monoclinic	Orthorhombic
Space group	$P\,2_1/n$ (no. 14)	$P\,2_12_12_1$ (no. 19)
Crystal colour and shape	Red block	Red rod
Crystal size	0.19 × 0.12 × 0.12	0.18 × 0.16 × 0.14
a (Å)	8.4123(4)	11.2492(10)
b (Å)	12.7708(5)	12.4866(9)
c (Å)	26.8982(12)	15.6083(13)
β (°)	94.9730(10)	90
V (Å^3)	2878.8(2)	2192.4(3)
Z	4	4
T (K)	173(2)	173(2)
D_c (g cm^{-3})	1.278	1.694
μ (mm^{-1})	0.703	6.220
Scan range (°)	$2.20 < \theta < 28.32$	$2.09 < \theta < 26.18$
Unique reflections	7169	4326
Observed refls [$I > 2\sigma(I)$]	5977	3811
R_{int}	0.0445	0.0553
Final R indices [$I > 2\sigma(I)$][a]	0.0439, wR_2 0.1273	0.0297, wR_2 0.0631
R indices (all data)	0.0541, wR_2 0.1360	0.0381, wR_2 0.0672
Goodness-of-fit	1.052	1.004
Max, Min $\Delta\rho/e$ (Å^{-3})	1.443, −0.738	1.138, −1.574

[a] Structures were refined on F_0^2: $wR_2 = [\sum[w(F_0^2 - F_c^2)^2]/\sum w(F_0^2)^2]^{1/2}$, where $w^{-1} = [\sum(F_0^2) + (aP)^2 + bP]$ and $P = [\max(F_0^2, 0) + 2F_c^2]/3$.

A2780cisR (cisplatin-resistant) cell lines. The mononuclear complexes **5** and **6** show moderate activity, with these complexes displaying better activity than the first-generation derivatives **1** and **2**. However, the octanuclear complexes are the most active of the series, with the second generation Rh-metallodendrimer **3** being the most active in the cisplatin-sensitive cell line (IC_{50} = 8.0 μM, A2780). All complexes display similar cytotoxicity in both the sensitive and resistant cell lines, suggesting a different mode of action to cisplatin. Furthermore, the second generation Ir-metallodendrimer **4** is the most active in the cisplatin-resistant cells (IC_{50} = 3.0 μM, A2780cisR). Notably, the activity of these metallodendrimers are comparable with the arene-ruthenium(II) complexes attached to similar dendritic scaffolds [33,39]. The correlation between the size dependency of the metallodendrimers and the cytotoxicity, which we previously reported for analogous mononuclear and higher generation polynuclear ruthenium complexes [33] and others observed too for related dinuclear complexes [41,42,48,49], is evident for complexes **1**–**6**.

Table 2
IC_{50} values of **1**–**6** on A2780 and A2780*cis*R human ovarian cancer cells, and HEK cells.

Compound	M	n[a]	A2780 (IC_{50}, μM)	A2780cisR (IC_{50}, μM)	HEK[b] (IC_{50}, μM)
1	Rh	4	>100	>100	>100
2	Ir	4	29.7 ± 0.1	28.1 ± 2.0	n.d.
3	Rh	8	8.0 ± 0.5	3.1 ± 0.3	4.5 ± 0.5
4	Ir	8	13.7 ± 0.1	3.0 ± 0.2	5.0 ± 1.2
5	Rh	1	13.4 ± 2.4	19.0 ± 1.2	52.9 ± 67.9
6	Ir	1	20.1 ± 13.6	19.0 ± 8.5	72.4 ± 91.1
Cisplatin	Pt	1	1.5	25	

n.d. = Not determined.
[a] n = Number of metals within the compound.
[b] IC_{50} values determined for the most active complexes against a normal, non-cancerous cell line.

Conclusions

A series of neutral, chelating, cyclometalated first- and second-generation Rh(III) and Ir(III) complexes based on poly(-propyleneimine) dendrimer scaffolds has been prepared and characterised. These compounds are air-stable and consequently their anticancer activity was evaluated *in vitro*. In general, the octanuclear chelating rhodium and iridium metallodendrimers show superior activity than analogous mononuclear rhodium and iridium complexes and comparable activity to ruthenium metallodendrimers reported previously. The generalisation, as noted before for ruthenium dendrimers that shows a correlation between the size dependency of the metallodendrimer and its cytotoxicity, is not always true for these rhodium and iridium complexes and one needs to go to the second-generation to get a slight improvement. Nonetheless, the most active compounds based on rhodium and iridium have comparable activities to the most active related ruthenium systems.

Experimental

General remarks

All synthetic procedures were performed under ambient conditions unless otherwise stated. All reagents were purchased from Sigma–Aldrich and used as received. Solvents were dried over Fluka Molecular Sieve dehydrate with indicator. Rh(III) and Ir(III) trichloride trihydrate was obtained from Johnson Matthey/Anglo American Platinum Limited. **L1** [50], $[Cp^*RhCl_2]_2$ [51] and $[Cp^*IrCl_2]_2$ [51] were synthesised following literature methods. Nuclear magnetic resonance (NMR) spectra were recorded on a Varian Unity XR400 spectrometer (^{1}H: 399.95 MHz; $^{13}C\{^1H\}$: 100.58 MHz; $^{31}P\{^1H\}$: 161.90 MHz) or Varian Mercury XR300 spectrometer (^{1}H: 300.08 MHz; $^{13}C\{^1H\}$: 75.46 MHz; $^{31}P\{^1H\}$: 121.47 MHz) or Bruker Biospin GmbH spectrometer (^{1}H: 400.22 MHz; $^{13}C\{^1H\}$: 100.65 MHz; $^{31}P\{^1H\}$: 162.00 MHz) at

ambient temperature using tetramethylsilane (TMS) as the internal standard. Infrared (IR) absorptions were measured on a Perkin–Elmer Spectrum One FT-IR spectrometer as KBr pellets. Elemental analysis (C, H, N) was carried out using a Thermo Flash 1112 Series CHNS–O Analyser. For certain metallodendrimers, the analyses are outside acceptable limits, and are ascribed to the encapsulation of solvent molecules and other inorganic salts by the dendritic compounds. Electrospray Ionisation (ESI) mass spectrometry was carried out on a Waters API Quattro Micro triple-quadrupole mass spectrometer in the positive-ion mode. Melting points were determined using a Büchi melting-point B-540 apparatus and are corrected.

General synthesis of the naphthaldimine dendrimers

The DAB-PPI-$(NH_2)_4$ (0.120 g, 0.373 mmol) or DAB-PPI-$(NH_2)_8$ (0.526 g, 0.680 mmol) dendritic scaffold was dissolved in ethanol (**G¹**: 10.0 mL; **G²**: 50.0 mL) followed by the addition of naphthaldehyde (**G¹**: 0.237 g, 1.52 mmol; **G²**: 0.853 g, 5.46 mmol). The reaction mixture was allowed to stir for 72–96 h after which the solvent was removed on a rotary evaporator and the residue was dissolved in DCM (30.0 mL) and washed with brine (15 × 30.0 mL). The organic layer was collected, dried over anhydrous $MgSO_4$ and then filtered by gravity. The solvent was removed on a rotary evaporator to yield the desired products as white solids.

*(**G¹**)*

White solid. Yield = 0.216 g (67%). IR (KBr pellet) ν(C=N) 1639 cm^{-1}. ^1H NMR (400 MHz, $CDCl_3$) δ (ppm) = 1.49 (m, 4H, NCH_2CH_2 core); 1.89 (m, 8H, $NCH_2CH_2CH_2N_{branch}$); 2.46 (br t, 4H, NCH_2CH_2 core); 2.57 (br t, 8H, $NCH_2CH_2CH_2N_{branch}$); 3.68 (br t, 8H, $NCH_2CH_2CH_2N_{branch}$); 7.47 (m, 8H, CH_{Ar}); 7.81 (br t, 12H, CH_{Ar}); 7.95 (m, 8H, CH_{Ar}); 8.40 (br d, 4H, CH_{imine}). Melting point: 104–108 °C. $^{13}C\{^1H\}$ NMR (100 MHz, $CDCl_3$) δ (ppm) = 25.25; 28.40; 51.74; 54.11; 59.74; 123.88; 126.36; 126.97; 127.83; 128.41; 128.57; 129.66; 133.14; 134.05; 134.64; 161.06. Elemental Analysis (%): Calc. For $C_{60}H_{64}N_6$ (869.21): C, 82.91; H, 7.42; N, 9.67; Found: C, 81.44; H, 7.78; N, 9.43. MS (LR-ESI, *m*/*z*): 322.20 $[M + 3H^+ + 3MeOH]^{3+}$.

*(**G²**)*

White solid. Yield = 0.842 g (66%). IR (KBr pellet) ν(C=N) 1639 cm^{-1}. ^1H NMR (400 MHz, $CDCl_3$) δ (ppm) = 1.33 (m, 4H, NCH_2CH_2 core); 1.53 (m, 8H, $NCH_2CH_2CH_2N_{1st\ branch}$); 1.80 (m, 16H, $NCH_2CH_2CH_2N_{2nd\ branch}$); 2.37 (overlapping m, 20H, NCH_2CH_2 core, $NCH_2CH_2CH_2N_{1st\ branch}$, $NCH_2CH_2CH_2N_{1st\ branch}$); 2.47 (br t, 16H, $NCH_2CH_2CH_2N_{2nd\ branch}$); 3.58 (br t, 16H, $NCH_2CH_2CH_2N_{2nd\ branch}$); 7.37 (m, 16H, CH_{Ar}); 7.70 (m, 24H, CH_{Ar}); 7.86 (m, 16H, CH_{Ar}); 8.36 (d, 8H, CH_{imine}). $^{13}C\{^1H\}$ NMR (100 MHz, $CDCl_3$) δ (ppm) = 24.75; 25.20; 28.48; 51.77; 52.37; 53.40; 54.26; 59.79; 123.88; 126.34; 126.95; 127.82; 128.39; 128.56; 129.67; 133.13; 134.05; 134.62; 160.99. Melting point: 64–67 °C. Elemental Analysis (%): Calc. For $C_{128}H_{144}N_{14}$ (1878.64): C, 81.84; H, 7.73; N, 10.44; Found: C, 80.54; H, 7.54; N, 10.37. MS (LR-ESI, *m*/*z*): 408.20 $[M + 5H^+ + MeOH]^{5+}$.

General synthesis of the metallodendrimers

The naphthaldimine dendrimer **G¹** (**1**: 0.0492 g, 0.0566 mmol; **2**: 0.0205 g, 0.0236 mmol) or dendrimer **G²** (**3**: 0.109 g, 0.0579 mmol; **4**: 0.121 g, 0.0645 mmol), sodium acetate (**1**: 0.0186 g, 0.227 mmol; **2**: 0.0081 g, 0.0987 mmol; **3**: 0.0386 g, 0.470 mmol; **4**: 0.0432 g, 0.527 mmol) and the $[Cp^*RhCl_2]_2$ (**1**: 0.0700 g, 0.113 mmol; **3**: 0.144 g, 0.232 mmol) or $[Cp^*IrCl_2]_2$ (**2**: 0.0376 g, 0.0472 mmol; **4**: 0.205 g, 0.258 mmol) dimer were stirred together in DCM or methanol (20.0 mL) for 24 h (for **1** and **2**) or for 48 h (for **3** and **4**) at room temperature, after which the reaction mixture was filtered through Celite and washed with DCM or methanol. The solvent was removed on a rotary evaporator to obtain the crude product. The solid was dissolved in a minimum amount of DCM, suspended in diethyl ether and placed in the fridge overnight. The following day a solid was observed, this was filtered under vacuum yielding the desired product as a light yellow–orange or red–orange solid.

*[$(Cp^*RhCl)_4$**G¹**] (**1**)*

Yellow–orange solid. Yield = 0.0605 g (52%). IR (KBr pellet) ν(C=N) 1609 cm^{-1}. ^1H NMR (400 MHz, $CDCl_3$) δ (ppm) = 1.57 (m, 4H, NCH_2CH_2 core); 1.61 (s, 60H, **Cp***); 1.70 (m, 8H, $NCH_2CH_2CH_2N_{branch}$); 2.20 (br t, 8H, $NCH_2CH_2CH_2N_{branch}$); 2.92 (m, 4H, NCH_2CH_2 core); 3.96 (splitting of br m, 8H, $NCH_2CH_2CH_2N_{branch}$); 7.30 (m, 8H, CH_{Ar}); 7.43 (m, 8H, CH_{Ar}); 7.74 (m, 8H, CH_{Ar}); 8.03 (s, 4H, CH_{imine}). $^{13}C\{^1H\}$ NMR (100 MHz, $CDCl_3$) δ (ppm) = 9.35; 23.56; 24.64; 26.25; 51.57; 59.72; 123.68; 123.74; 126.50; 126.93; 128.30; 128.77; 130.48; 133.37; 135.60; 135.64; 145.66. Melting point: 220–224 °C. Elemental Analysis (%): Calc. For $C_{100}H_{120}Cl_4N_6Rh_4$ (1959.54): C, 61.29; H, 6.17; N, 4.29; Found: C, 61.17; H, 6.02; N, 4.93. MS (HR-ESI, *m*/*z*): 1923.4751 $[M - Cl]^+$; 1959.4369 $[M]^+$.

*[$(Cp^*IrCl)_4$**G¹**] (**2**)*

Yellow–orange solid. Yield = 0.0230 g (42%). IR (KBr pellet) ν(C=N) 1602 cm^{-1}. ^1H NMR (400 MHz, $CDCl_3$) δ (ppm) = 1.50 (m, 8H, $NCH_2CH_2CH_2N_{branch}$); 1.75 (m, 8H, NCH_2CH_2 core); 1.65 (s, 60H, **Cp***); 2.11 (m, 4H, NCH_2CH_2 core); 2.49 (br m, 8H, $NCH_2CH_2CH_2N_{branch}$); 4.12 (m, 8H, $NCH_2CH_2CH_2N_{branch}$); 7.26 (br t, 8H, CH_{Ar}); 7.39 (br t, 8H, CH_{Ar}); 7.73 (br t, 8H, CH_{Ar}); 8.02 (br t, 8H, CH_{Ar}); 8.29 (br s, 4H, CH_{imine}). $^{13}C\{^1H\}$ NMR (100 MHz, $CDCl_3$) δ (ppm) = 9.15; 25.64; 26.35; 28.16; 51.60; 60.96; 122.87; 123.40; 126.47; 126.98; 128.88; 130.09; 131.87; 136.60; 141.18; 141.37; 146.27. Melting point: 226–232 °C. Elemental Analysis (%): Calc. for $C_{100}H_{120}Cl_4Ir_4N_6$ (2316.78): C, 51.84; H, 5.22; N, 3.63; Found: C, 51.10; H, 5.31; N, 3.16. MS (HR-ESI, *m*/*z*): 1122.3962 $[M - 2Cl]^{2+}$, 1159.3489 $[M + 2H]^{2+}$.

*[$(Cp^*RhCl)_8$**G²**] (**3**)*

Red–orange solid. Yield = 0.240 g (80%). IR (KBr pellet) ν(C=N) 1610 cm^{-1}. ^1H NMR (400 MHz, $CDCl_3$) δ (ppm) = 0.8 (m, 4H, NCH_2CH_2 core); 1.18 (m, 8H, $NCH_2CH_2CH_2N_{1st\ branch}$); 1.56 (s, 120H, **Cp***); 1.89 (br m, 16H, $NCH_2CH_2CH_2N_{2nd\ branch}$); 2.20 (br m, 36H, NCH_2CH_2 core, $NCH_2CH_2CH_2N_{1st\ branch}$, $NCH_2CH_2CH_2N_{1st\ branch}$, $NCH_2CH_2CH_2N_{2nd\ branch}$): 3.97 (splitting, 16H, $NCH_2CH_2CH_2N_{2nd\ branch}$); 7.20 (m, 16H, CH_{Ar}); 7.34 (m, 8H, CH_{Ar}); 7.65 (m, 16H, CH_{Ar}); 7.88 (m, 8H, CH_{Ar}); 7.93 (br s, 8H, CH_{imine}). $^{13}C\{^1H\}$ NMR (100 MHz, $CDCl_3$) δ (ppm) = 9.41; 10.70; 12.80; 26.00; 45.88; 51.83; 52.97; 54.16; 59.90; 93.20; 95.70; 123.73; 125.0; 126.43; 126.91; 128.22; 128.83; 130.48; 135.52; 143.36. Melting point: 178–180 °C. Elemental Analysis (%): Calc. for $C_{208}H_{256}Cl_8N_{14}Rh_8$ (4059.27 g/mol): C, 61.54; H, 6.36; N, 4.83; Found: C, 60.76; H, 6.46; N, 4.45. MS (HR-ESI, *m*/*z*): 640.9327 $[M - 6Cl]^{6+}$.

*[$(Cp^*IrCl)_8$**G²**] (**4**)*

Red–orange solid. Yield = 0.243 g (79%). IR (KBr pellet) ν(C=N) 1600 cm^{-1}. ^1H NMR (400 MHz, $CDCl_3$) δ (ppm) = 1.40 (m, 4H, NCH_2CH_2 core); 1.48 (m, 8H, $NCH_2CH_2CH_2N_{1st\ branch}$); 1.60 (s, 120H, **Cp***); 1.86 (br m, 16H, $NCH_2CH_2CH_2N_{2nd\ branch}$); 1.94 (br m, 36H, NCH_2CH_2 core, $NCH_2CH_2CH_2N_{1st\ branch}$, $NCH_2CH_2CH_2N_{1st\ branch}$); 2.50 (br m, 16H, $NCH_2CH_2CH_2N_{2nd\ branch}$); 4.00 (br m, 16H, $NCH_2CH_2CH_2N_{2nd\ branch}$); 7.32 (m, 16H, CH_{Ar}); 7.65 (m, 8H, CH_{Ar}); 7.93 (m, 16H, CH_{Ar}); 8.45 (br s, 8H, CH_{imine}). $^{13}C\{^1H\}$ NMR (100 MHz, $CDCl_3$) δ (ppm) = 9.17; 20.97; 24.33; 29.15; 51.11–53.19; 60.86; 126.43; 127.08; 127.65; 128.99; 130.04; 131.9; 134.86; 136.55; 146.98. Melting point: 180–182 °C. Elemental Analysis (%): Calc. for $C_{208}H_{256}Cl_8Ir_8N_{14}$ (4773.79 g/mol): C, 52.33; H, 5.40; N, 4.11; Found:

C, 51.460; H, 5.27; N, 4.54. MS (HR-ESI, *m/z*): 761.7429 $[M - 6Cl]^{6+}$; 1152.3954 $[M - 4Cl]^{4+}$.

Synthesis of the mononuclear complexes

The naphthaldimine ligand **L1** (**5**: 0.0409 g, 0.207 mmol; **6**: 0.0408 g, 0.207 mmol), sodium acetate (**5**: 0.0339 g, 0.413 mmol; **6**: 0.0343 g, 0.418 mmol) and the $[Cp^*RhCl_2]_2$ (0.0634 g, 0.102 mmol) or $[Cp^*IrCl_2]_2$ (0.0810 g, 0.102 mmol) dimer were stirred together in DCM or methanol (20.0 mL) for 2 h at room temperature. The reaction mixture was filtered through Celite, washing with DCM or methanol. The solvent was removed to obtain the crude product. This was then washed with diethyl ether to obtain the desired product as an orange–red (**5**) or orange–brown (**6**) solid. The Rh(III) complex **5** was recrystallised from toluene and hexane by slow evaporation and the Ir(III) complex **6** was recrystallised from methanol and hexane.

*[Cp*RhCl**L1**] (**5**)*

Orange–red solid. Yield = 0.0480 g (50%). IR (KBr pellet) ν(C=N) 1610 cm^{-1}. ^1H NMR (400 MHz, $CDCl_3$) δ (ppm) = 1.01 (t, ^3J = 7.4 Hz, 3H, $NCH_2CH_2C\mathbf{H}_3$); 1.69 (s, 15H, **Cp***); 1.93 (m, 1H, $NCH_2C\mathbf{H}_2CH_3$); 2.11 (m, 1H, $NCH_2C\mathbf{H}_2CH_3$); 3.72 (m, 1H, $NC\mathbf{H}_2CH_2CH_3$); 4.12 (m, 1H, $NC\mathbf{H}_2CH_2CH_3$); 7.29 (t, ^3J = 6.9 Hz, 1H, $C\mathbf{H}_{Ar}$); 7.44 (t, ^3J = 6.8 Hz, 1H, $C\mathbf{H}_{Ar}$); 7.74 (m, 2H, $C\mathbf{H}_{Ar}$); 7.90 (s, 1H, $C\mathbf{H}_{Ar}$); 8.06 (s, 1H, $C\mathbf{H}_{Ar}$); 8.23 (s, 1H, $C\mathbf{H}_{imine}$). $^{13}C\{^1H\}$ NMR (100 MHz, $CDCl_3$) δ (ppm) = 11.75; 63.98; 95.70; 123.84; 126.60; 127.06; 128.70; 129.16; 129.57; 130.50; 134.63; 135.68; 145.21; 171.69; 192.35. Melting point: 168–170 °C. Elemental Analysis (%): Calc. For $C_{24}H_{29}ClNRh$ (469.86): C, 61.35; H, 6.22; N, 2.98; Found: C, 61.81; H, 6.16; N, 2.58. MS (LR-ESI, *m/z*): 434.23 $[M - Cl]^+$.

*[Cp*IrCl**L1**] (**6**)*

Orange–brown solid. Yield = 0.0800 g (71%). IR (KBr pellet) ν(C=N) 1603 cm^{-1}. ^1H NMR (400 MHz, $CDCl_3$) δ (ppm) = 1.03 (t, ^3J = 7.2 Hz, 3H, $NCH_2CH_2C\mathbf{H}_3$); 1.80 (s, 15H, **Cp***); 1.98 (m, 1H, $NCH_2C\mathbf{H}_2CH_3$); 2.12 (m, 1H, $NCH_2C\mathbf{H}_2CH_3$); 3.93 (m, 1H, $NC\mathbf{H}_2CH_2CH_3$); 4.11 (m, 1H, $NC\mathbf{H}_2CH_2CH_3$); 7.27 (t, ^3J = 6.8 Hz, 1H, $C\mathbf{H}_{Ar}$); 7.42 (t, ^3J = 6.7 Hz, 1H, $C\mathbf{H}_{Ar}$); 7.74 (m, 2H, $C\mathbf{H}_{Ar}$); 8.01 (s, 1H, $C\mathbf{H}_{Ar}$); 8.06 (s, 1H, $C\mathbf{H}_{Ar}$); 8.44 (s, 1H, $C\mathbf{H}_{imine}$). $^{13}C\{^1H\}$ NMR (100 MHz, $CDCl_3$) δ (ppm) = 22.77; 65.23; 88.51; 123.50; 126.57; 127.07; 128.37; 128.83; 130.10; 132.06; 136.60; 145.21; 171.69; 192.35. Melting point: 206–208 °C. Elemental Analysis (%): Calc. For $C_{24}H_{29}ClIrN$ (559.17): C, 51.55; H, 5.23; N, 2.50; Found: C, 51.83; H, 5.35; N, 2.63. MS (LR-ESI, *m/z*): 524.40 $[M - Cl]^+$.

Single-crystal X-ray structure analyses

Single-crystal X-ray diffraction data for complex **5** were collected on a Bruker KAPPA APEX II DUO diffractometer using graphite-monochromated MoKα radiation (χ = 0.71073 Å). Data collection was carried out at 173(2) K. Temperature was controlled by an Oxford Cryostream cooling system (Oxford Cryostat). Cell refinement and data reduction were performed using the program SAINT [52]. The data were scaled and absorption correction performed using SADABS[2]. The structure was solved by direct methods using SHELXS-97[2] and refined by full-matrix least-squares methods based on F^2 using SHELXL-97 [53] and using the graphics interface program X-Seed [54,55]. All non-hydrogen atoms, except those of the solvent molecule, were refined anisotropically. All hydrogen atoms, except those of the solvent molecule, were placed in idealised positions and refined with geometrical constraints. The solvent is found to be toluene with methyl carbon disordered over two positions (C31A and C31B) with each having site occupancy factor of 0.50. The solvent molecule exhibit high thermal motions and were refined with isotropic temperature factors and the phenol ring was fitted to a regular pentagon. The hydrogen atoms of the solvent molecule were excluded in the structure model. Crystallographic details are summarised in Table 1.

Crystal of complex **6** was mounted on a Stoe Image Plate Diffraction system equipped with a ϕ circle goniometer, using MoKα graphite monochromated radiation (λ = 0.71073 Å) with ϕ range 0–200°. The structure was solved by direct methods using the program SHELXS-97, while the refinement and all further calculations were carried out using SHELXL-97 [14]. The H-atoms were included in calculated positions and treated as riding atoms using the SHELXL default parameters. The non-H atoms were refined anisotropically, using weighted full-matrix least-square on F^2. Crystallographic details are summarized in Table 1. Fig. 2 was drawn with ORTEP [56].

Cytotoxicity study

The human A2780 and A2780cisR ovarian carcinoma cell lines were obtained from the European Collection of Cell Cultures (Salisbury, UK). Cells were grown routinely in RPMI-1640 medium with 10% foetal calf serum (FCS) and antibiotics at 37 °C and 5% CO_2. Cytotoxicity was determined using the MTT assay (MTT = 3(4,5 dimethyl 2-thiazolyl)-2,5-diphenyl-2H-tetrazolium bromide). Cells were seeded in 96-well plates as monolayers with 100 µL of cell solution (approximately 20,000 cells) per well and pre-incubated for 24 h in medium supplemented with 10% FCS. Compounds were prepared as DMSO solution then dissolved in the culture medium and immediately serially diluted to the appropriate concentration, to give a final DMSO concentration of 0.5%. A 100 µL portion of drug solution was added to each well and the plates were incubated for another 72 h. Subsequently, MTT (5 mg/mL solution) was added to the cells and the plates were incubated for a further 2 h. The culture medium was aspirated, and the purple formazan crystals formed by the mitochondrial dehydrogenase activity of vital cells were dissolved in DMSO. The optical density, directly proportional to the number of surviving cells, was quantified at 590 nm using a multiwell plate reader and the fraction of surviving cells was calculated from the absorbance of untreated control cells. Evaluation is based on means from two independent experiments, each comprising three microcultures per concentration level.

Acknowledgements

Financial support from the University of Cape Town, the National Research Foundation (NRF) of South Africa (UID: 66054), and a generous loan of rhodium and iridium trichloride from Johnson Matthey/Anglo American Platinum Limited Corporation are gratefully acknowledged. The Swiss-South African Joint Research Programme is also thanked for a short-term exchange grant between the three laboratories.

Appendix A. Supplementary material

CCDC 1018362 **5**·toluene and 1025190 **6** contain the supplementary crystallographic data for this paper. These data can be obtained free of charge from The Cambridge Crystallographic Data Centre via www.ccdc.cam.ac.uk/data_request/cif.

References

[1] C.X. Zhang, S.J. Lippard, Curr. Opin. Chem. Biol. 7 (2003) 481–489.
[2] L. Ronconi, P.J. Sadler, Coord. Chem. 251 (2007) 1633–1648.
[3] C. Orvig, M.J. Abrams, Chem. Rev. 99 (1999) 2201–2203.
[4] C.S. Allardyce, A. Dorcier, C. Scolaro, P.J. Dyson, Appl. Organomet. Chem. 19 (2005) 1–10.

[5] G. Gasser, I. Ott, N.J. Metzler-Nolte, Med. Chem. Res. 54 (2011) 3–25.
[6] G. Jaouen, in: Wiley-VCH, Weinheim, 2006.
[7] P.J. Dyson, G. Sava, Dalton Trans. 16 (2006) 1929–1933.
[8] C.J. Jones, in: J.R. Thornback (Ed.), Medicinal Application of Coordination Chemistry, RSC Publishing, Cambridge, 2007.
[9] G. Jaouen, N. Metzler-Nolte, Medicinal Organometallic Chemistry, Springer-Verlag, Heidelberg, Germany, 2010.
[10] R.H. Fish, Aust. J. Chem. 63 (2010) 1505–1513.
[11] P.C.A. Bruijnincx, P.J. Sadler, in: R. van Eldik (Ed.), Advances in Inorganic Chemistry, Academic Press, New York, 2009, pp. 1–62.
[12] N.J. Wheate, S. Walker, G.E. Craig, R. Oun, Dalton Trans. 39 (2010) 8097–8340.
[13] M.A. Jakupec, M. Galanski, V.B. Arion, C.G. Hartinger, B.K. Keppler, Dalton Trans. (2008) 183–194.
[14] W.H. Ang, P.J. Dyson, Eur. J. Inorg. Chem. 20 (2006) 4003–4018.
[15] A. Bergamo, G. Sava, Dalton Trans. 13 (2007) 1267–1272.
[16] C.G. Hartinger, P.J. Dyson, Chem. Soc. Rev. 38 (2009) 391–401.
[17] C.G. Hartinger, M.A. Jakupec, S. Zorbas-Seifried, M. Groessl, A. Egger, W. Berger, H. Zorbas, P.J. Dyson, B.K. Keppler, Chem. Biodiversity 5 (2008) 2140–2155.
[18] C.G. Hartinger, S. Zorbas-Seifried, M.A. Jakupec, B. Kynast, H. Zorbas, B.K. Keppler, J. Inorg. Biochem. 100 (2006) 891–904.
[19] G.E. Büchel, I.N. Stepanenko, M. Hejl, M.A. Jakupec, B.K. Keppler, V.B. Arion, Inorg. Chem. 50 (2011) 7690–7697.
[20] Y. Fu, A. Habtemariam, A.M. Pizarro, S.H. van Rijt, D.J. Healey, P.A. Cooper, S.D. Shnyder, G.J. Clarkson, P.J. Sadler, J. Med. Chem. 53 (2010) 8192–8196.
[21] M. Hanif, A.A. Nazarov, C.G. Hartinger, W. Kandioller, M.A. Jakupec, V.B. Ario, P.J. Dyson, B.K. Keppler, Dalton Trans. 39 (2010) 7345–7352.
[22] S.H. Van Rijt, A.F.A. Peacock, R.D.L. Johnstone, S. Parsons, P.J. Sadler, Inorg. Chem. 48 (2009) 1753–1762.
[23] S.H. Van Rijt, A. Mukherjee, A.M. Pizarro, P.J. Sadler, J. Med. Chem. 53 (2010) 840–849.
[24] A. Dorcier, C.G. Hartinger, R. Scopelliti, R.H. Fish, B.K. Keppler, P.J. Dyson, J. Inorg. Biochem. 102 (2008) 1066–1076.
[25] L.K. Filak, G. Muhlgassner, F. Bacher, A. Roller, M. Galanski, M.A. Jakupec, B.K. Keppler, V.B. Ario, Organometallics 30 (2011) 273–283.
[26] R. Schuecker, R.O. John, M.A. Jakupec, V.B. Arion, B.K. Keppler, P.J. Dyson, Organometallics 27 (2008) 6587–6597.
[27] M.B. Schwarz, A. Kurzwernhart, A. Roller, W. Kandioller, B.K. Keppler, C.G. Hartinger, Z Anorg. Allg. Chem., 639 1648–1654.
[28] O. Dömötör, S. Aicher, M. Schmidlehner, M.S. Novak, A. Roller, M.A. Jakupec, W. Kandioller, C.G. Hartinger, B.K. Keppler, E.A. Enyedy, J. Inorg. Biochem. 134 (2014) 57–65.
[29] Z. Liu, P.J. Sadler, Acc. Chem. Res. 47 (2014) 1174–1185.
[30] C.-H. Leung, H.-J. Zhong, D.S.-H. Chan, D.-L. Ma, Coord. Chem. Rev. 257 (2013) 1764–1776.
[31] N. Cutillas, G.S. Yellol, C. de Haro, C. Vicente, V. Rodriguez, J. Ruiz, Coord. Chem. Rev. 257 (2013) 2784–2797.
[32] P. Govender, N.C. Antonels, J. Mattsson, A.K. Renfrew, P.J. Dyson, J.R. Moss, B. Therrien, G.S. Smith, J. Organomet. Chem. 694 (2009) 3470–3476.
[33] P. Govender, A.K. Renfrew, C.M. Clavel, P.J. Dyson, B. Therrien, G.S. Smith, Dalton Trans. 40 (2011) 1158–1167.
[34] T. Kapp, A. Dullin, R. Gust, J. Med. Chem. 49 (2006) 1182–1190.
[35] X. Zhao, A.C.J. Loo, P.P.-F. Lee, T.T.Y. Tan, C.K. Chu, J. Inorg. Biochem.. 104 (2010) 105–110.
[36] C. Billecke, S. Finniss, L. Tahash, C. Miller, T. Mikkelsen, N.P. Farrell, O. Bogler, Neuro-Oncology 8 (2006) 215–226.
[37] P. Govender, B. Therrien, G.S. Smith, Eur. J. Inorg. Chem. (2012) 2853–2862.
[38] P. Govender, F. Edafe, B.C.E. Makhubela, P.J. Dyson, B. Therrien, G.S. Smith, Inorg. Chim. Acta 409 (2014) 112–120.
[39] P. Govender, L.C. Sudding, C.M. Clavel, P.J. Dyson, B. Therrien, G.S. Smith, Dalton Trans. 42 (2013) 1267–1277.
[40] R. Payne, P. Govender, B. Therrien, C.M. Clavel, P.J. Dyson, G.S. Smith, J. Organomet. Chem. 729 (2013) 20–27.
[41] M.G. Mendoza-Ferri, C.G. Hartinger, M.A. Mendoza, M. Groessl, A. Egger, R.E. Eichinger, J.B. Mangrum, N.P. Farrell, M. Maruszak, P.J. Bednarski, F. Klein, M.A. Jakupec, A.A. Nazarov, K. Severin, B.K. Keppler, J. Med. Chem. 52 (2009) 916–925.
[42] M.G. Mendoza-Ferri, C.G. Hartinger, R. Eichinger, N. Stolyarova, K. Severin, M.A. Jakupec, A.A. Nazarov, B.K. Keppler, Organometallics 27 (2008) 2405–2407.
[43] M. Auzias, J. Gueniat, B. Therrien, G. Süss-Fink, A.K. Renfrew, P.J. Dyson, J. Organomet. Chem. 694 (2009) 855–861.
[44] N. Farrell, Met. Ions Biol. Syst. 42 (2004) 251–296.
[45] A. Casini, M.A. Cinellu, G. Minghetti, C. Gabbiani, M. Coronnello, E. Mini, L. Messori, J. Med. Chem. 49 (2006) 5524–5531.
[46] C. Gabbiani, A. Casini, L. Messori, A. Guerri, M.A. Cinellu, G. Minghetti, M. Corsini, C. Rosani, P. Zanello, M. Arca, Inorg. Chem. 47 (2008) 2368–2379.
[47] M.A. Cinellu, L. Maiore, M. Manassero, A. Casini, M. Arca, H.H. Fiebig, G. Kelter, E. Michelucci, G. Pieraccini, C. Gabbiani, L. Messori, Med. Chem. Lett. 1 (2010) 336–339.
[48] M.G. Mendoza-Ferri, C.G. Hartinger, A.A. Nazarov, R.E. Eichinger, M.A. Jakupec, K. Severin, B.K. Keppler, Organometallics 28 (2009) 6260–6265.
[49] O. Nováková, A.A. Nazarov, C.G. Hartinger, B.K. Keppler, V. Brabec, Biochem. Pharmacol. 77 (2009) 364–374.
[50] N. Mungwe, A.J. Swarts, S.F. Mapolie, G. Westman, J. Organomet. Chem. 696 (2011) 3527–3535.
[51] C. White, A. Yates, P.M. Maitlis, Inorg. Synth. 29 (1992) 228–234.
[52] G.M. Sheldrick, SAINT Version 7.60a, Brucker AXS Inc., Madison, WI, USA, 2006.
[53] G.M. Sheldrick, Acta Crystallogr. A64 (2008) 112–122.
[54] L.J. Barbour, J. Supramol. Chem. 1 (2001) 189–191.
[55] J.L. Atwood, L.J. Barbour, Cryst. Growth Des. 3 (2003) 3–8.
[56] L. Farrugia, J. Appl. Crystallogr. 30 (1997) 565.